



# Study of Renewable Silica Powder Influence in the Preparation of Bioplastics from Corn and Potato Starch

Luciana C. de Azêvedo<sup>1,2</sup> · Suzimara Rovani<sup>2</sup> · Jonnatan J. Santos<sup>3</sup> · Djalma B. Dias<sup>2</sup> · Sandi S. Nascimento<sup>1</sup> · Fábio F. Oliveira<sup>4</sup> · Leonardo G. A. Silva<sup>2</sup> · Denise A. Fungaro<sup>2</sup>

Accepted: 29 September 2020 / Published online: 8 October 2020  
© Springer Science+Business Media, LLC, part of Springer Nature 2020

## Abstract

In the present study, 0.5–1.5% silica powder, from sugarcane waste ash, was incorporated into corn and potato starch bioplastics doped with sodium silicate solution to improve the properties of elongation at break and increase the thermal resistance of the bioplastics. The starch-based bioplastics were produced by casting and characterized by color analyses, transparency, opacity apparent, humidity, thickness, tensile strength, elongation at break, FTIR, DSC, SEM, and biodegradation assay. The addition of 0.5% of silica powder improved the elongation at break of the corn starch-based bioplastics. The sample CS5-P0.5 presented the highest percentage of elongation at the break among the studied samples, increased from 59.2% (without silica powder) to 78.9% (with silica powder). For potato starch bioplastic the addition of 0.5% of silica powder did not improve elongation at break but increased the thermal resistance. Increased until 17 °C for PS5-P0.5 sample and until 11 °C for PS7.5-P0.5 sample. The bioplastics of potato starch were biodegraded in 5 days, and those of corn starch took almost 40 days. Silica powder inhibited the growth of fungi in starch bioplastics.

---

**Electronic supplementary material** The online version of this article (<https://doi.org/10.1007/s10924-020-01911-8>) contains supplementary material, which is available to authorized users.

---

✉ Luciana C. de Azêvedo  
luciana.cavalcanti@ifsertao-pe.edu.br

✉ Suzimara Rovani  
suzimara.rovani@ipen.br; suzirovani@gmail.com

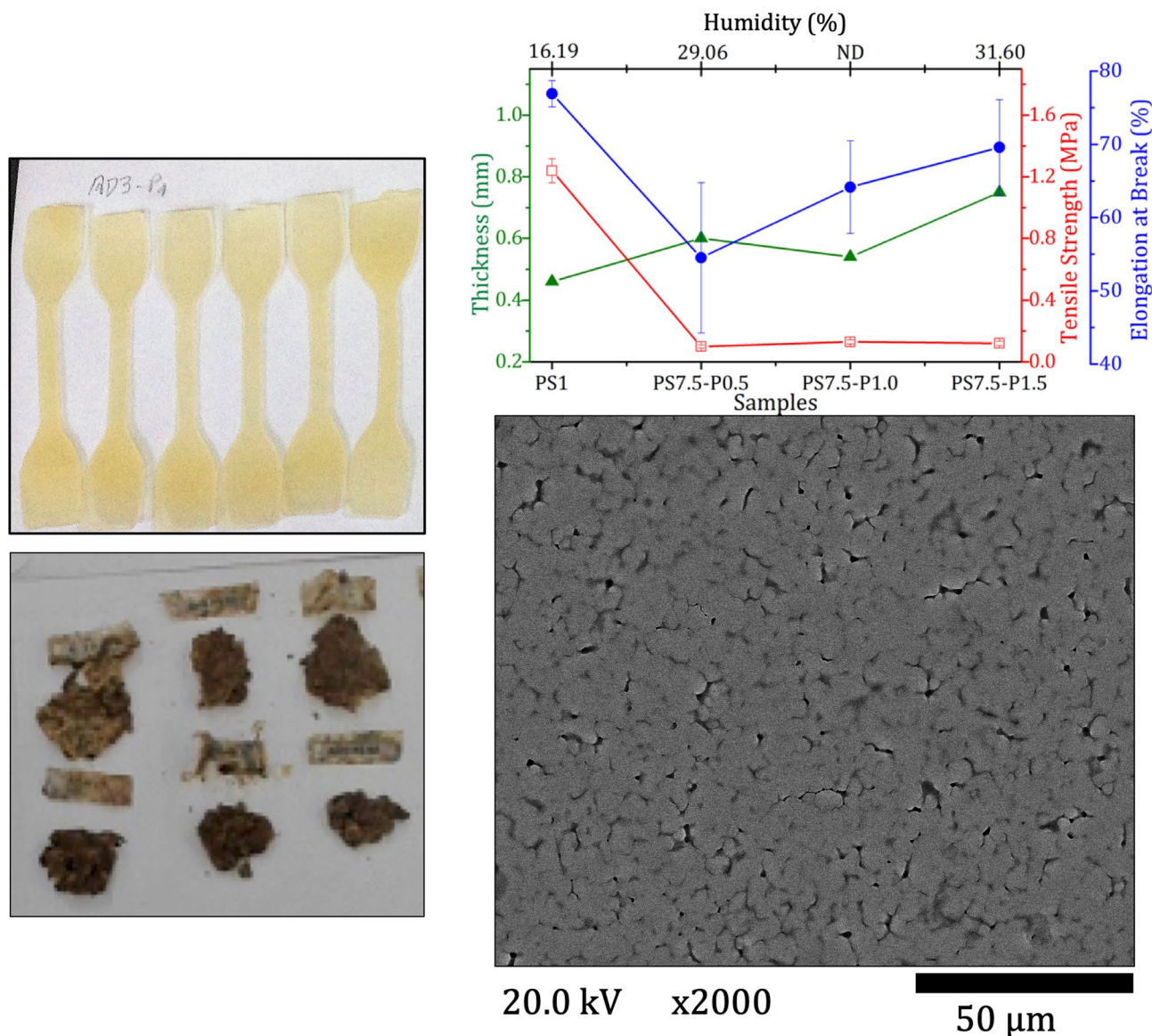
<sup>1</sup> Department of Food Technology, Federal Institute - IF SERTAO-PE, BR 407, Km 08, Jardim São Paulo, Petrolina, PE CEP: 56314-520, Brazil

<sup>2</sup> Instituto de Pesquisas Energéticas e Nucleares (IPEN-CNEN/SP), Avenida Professor Lineu Prestes, 2242, Cidade Universitária, São Paulo, SP CEP: 05508-000, Brazil

<sup>3</sup> Instituto de Química, Universidade de São Paulo, Avenida Professor Lineu Prestes, 748, Cidade Universitária, São Paulo, SP CEP: 05508-000, Brazil

<sup>4</sup> Departamento de Ciências Agrárias/Solos, Federal Institute - IF SERTAO-PE, BR 235, Km 22, Zona Rural, Petrolina, PE CEP: 56302-970, Brazil

## Graphic Abstract



**Keywords** Bioplastics · Sugarcane waste ash · Corn starch · Potato starch · Silica

## Introduction

Scientists around the world are studying the impacts of oil-derived plastics on planet Earth. Some studies say that if nothing is done in 2050, there will be more plastics than fish in the oceans. But not only the life in oceans is affected, but birds are also dying from eating plastics by mistake. Changes in the plastics manufacturing and use process need urgently to be reviewed [1–3].

Bioplastics, in the turn, are in high trend as they are generally biodegradable, show a rational use of natural

resources, and reduce environmental pollution. Starch-based bioplastics have some advantages, such as low cost, renewability, biodegradability, and ease of processing [4]. Many researchers have investigated the preparation of starch-based bioplastics using different types of starch, such as potato starch [5–7], cassava starch [6, 8, 9], corn starch [6, 9, 10], pinhão starch [11], Jicama (*Pachyrhizus erosus*) starch [12], wheat starch [13, 14], and jackfruit seed starch [15]. These starch-based bioplastics are exploited as a promising type of commercially preserved bioplastics to extend the shelf life of food [16]. However,

starch-based bioplastics have some disadvantages, including low thermal resistance and poor mechanical properties [17].

In this way, composite materials containing nanoparticles inorganics can generate innovative high-performance materials. The inorganic nanoparticles keep exceptional interfacial interactions in bioplastics, and significantly improve their properties. According to literature, all mechanical and thermal properties of bioplastic composites improve with the addition of nanoparticles inorganics [5, 18, 19].

Wu et al. [20] studied the effect of silica nanoparticles on the wear performance and tensile strength of starch films. They observed that the best results were obtained when the silica content was 3–4%. They also noted that if the diameter of the silica nanoparticles were smaller, the performance of the starch film would be improved. Yao et al. [18] reported that the properties of starch-based bioplastic with the addition of silica nanoparticles have been improved. Intermolecular hydrogen bonds were formed between silica nanoparticles and corn starch. Ghazihoseini et al. [19] also observed that the incorporation of silica nanoparticles improved the thermal sealability and the mechanical properties of films made of soluble soya polysaccharide.

Zhang et al. [5] demonstrated that the size of the silica nanoparticles played an important role in the physical performance and mechanical properties of potato starch films. The 100 nm silica nanoparticles were uniformly dispersed and there was an improvement in the mechanical properties of the potato starch bioplastics.

Most recently, Datta and Halder [21] studied the production of silica from rice husk and the incorporation of this silica in the corn-starch/LDPE composites matrix. The addition of silica led to the improvement of the mechanical properties. However, an increase in the silica content of more than 1.5% decreased the tensile strength due to its greater agglomerating nature.

Within this context, in the present study, we prepared silica from sugarcane waste ash and incorporated this silica in corn and potato starch bioplastics doped with sodium silicate solution. To improve the properties of elongation at break and increase the thermal resistance of the bioplastics, we studied the incorporation of 0.5–1.5% silica powder.

## Experimental Part

### Materials and Methods

#### Materials and Reagents

All aqueous solutions were prepared using deionized water, with resistivity higher than 18.2 M $\Omega$  cm, obtained from a MilliQ deionizer, model Elix Millipore. Sugarcane

waste ash was kindly donated by COSAN S.A. Sodium hydroxide micro-pearls (> 99%), hydrochloric acid (35–37%) were purchased from Synth, Brazil. Glycerol ( $\geq 99.5\%$ ) was obtained from Sigma-Aldrich, Brazil. Corn starch was purchased from Unilever Brazil Industrial, and potato starch was purchased from Dinâmica Química Contemporânea Ltda, Brazil.

#### Synthesis of Silica Powder Using Sodium Silicate Extracted from the Sugarcane Waste Ash

The sodium silicate was extracted from the sugarcane waste ash, according to the methodology described in previously published articles [22–24]. After the extraction of sodium silicate, a hydrochloric acid solution ( $[HCl] = 3 \text{ mol L}^{-1}$ ) was slowly added to the sodium silicate solution [23, 24], obtained from sugarcane waste ash until  $pH = 7$  for complete precipitation of amorphous silica. Then, the formed silica gel was filtered, washed, and dried at 105 °C, in an oven for 12 h, and sieving in a 100 mesh (150  $\mu\text{m}$ ) [25].

#### Casting of Bioplastics

Briefly, the filmogenic solution was prepared by dissolving corn starch or potato starch in a solution of HCl (0.10 mol  $\text{L}^{-1}$ ), under stirring and heating for 30 min. Glycerol and silica powder were added to the mixture when the temperature reached 55 and 65 °C, respectively.

The filmogenic solution was prepared with 10.0% of starch, 6.0% of HCl (0.1 mol  $\text{L}^{-1}$ ), 4.0% of sodium silicate solution at 15.5%, 5.0–7.5% of glycerol, and 0–1.5% of silica powder. The samples prepared with corn starch and potato starch were named CS and PS, respectively. Samples with the addition of silica powder were named “P” for example, P0.5, P1.0, and P1.5 (0.5, 1.0, and 1.5% of silica powder, respectively). The samples CS1 and PS1 are without sodium silicate and silica, and with 0.10 mol  $\text{L}^{-1}$  NaOH solution were used as control bioplastics samples [22]. Table 1 are presented the name of the samples and the parameters changed in every sample.

## Characterization

### Fourier Transform Infrared Spectroscopy (FTIR)

Fourier transform infrared spectroscopy was performed using a Spectrometer from Bruker, model Alpha, operating in an attenuated total reflectance mode (ATR). The spectra were obtained using 200 cumulative scans, in the range from 375 to 4000  $\text{cm}^{-1}$ .

**Table 1** Description of the reagents used for the preparation of bioplastics from corn starch (CS) or potato starch (PS)

Bioplastics	Sodium silicate solution (%) <sup>*</sup>	Glycerol (%) <sup>*</sup>	Silica powder (%) <sup>*</sup>
CS1 and PS1	NaOH (0.1 mol L <sup>-1</sup> )	5.0	0
CS5-P0.5 and PS5-P0.5	4.0	5.0	0.5
CS5-P1.0 and PS5-P1.0	4.0	5.0	1.0
CS5-P1.5 and PS5-P1.5	4.0	5.0	1.5
CS7.5-P0.5 and PS7.5-P0.5	4.0	7.5	0.5
CS7.5-P1.0 and PS7.5-P1.0	4.0	7.5	1.0
CS7.5-P1.5 and PS7.5-P1.5	4.0	7.5	1.5

<sup>\*</sup>Percentages calculated on the volume of the filmogenic solution

### Differential Scanning Calorimetry (DSC)

DSC curves were obtained using an equipment model DSC 822e from Mettler Toledo. The dry samples (~40.0 mg) were analyzed under the nitrogen atmosphere, with a flow of 30 mL min<sup>-1</sup>, using an aluminum-pan sample heated until 250 °C with a heating rate of 10 °C min<sup>-1</sup>.

### Scanning Electron Microscopy (SEM)

SEM images were obtained using a tabletop microscope from QUANTA FEG 650, from Thermo Fischer Scientific, Oregon, EUA. Before the SEM analyses, the samples were fixed on the sample holder with carbon tape and covered by a thin film of gold using a BalTec Sample Coater/Sputter, Model SCD 050.

### Mechanical Properties

The mechanical properties of the starch-based bioplastic were analyzed as described previously [22]. Briefly, three or more specimens, with a size of 73 × 12 mm, were cut from each bioplastic. The samples were conditioned at 25 °C and 46% RH for 72 h, and the thickness of the samples was measured with a micrometer (INSIZE, 3109-25, São Paulo, Brazil) before the test. Measurements were taken at five different positions for each sample, and the average value of these determinations was calculated. This average value was used to calculate the cross-sectional area of the samples (the area is equal to the thickness multiplied by the width of each sample). The tensile strength and percent elongation at break were measured using an electromechanical universal testing machine (Instron, 5567, São José dos Pinhais, Paraná, Brazil), using a calibrated 1 kN (100 kg) load cell, according to ASTM Standard Method ASTM D882-12 and ASTM D638-14, with some adaptations. The initial grip separation was 45 mm, and the cross-head speed was 50 mm min<sup>-1</sup>. The tensile strength was calculated by dividing the maximum force exerted on the bioplastic during fracture by the cross-sectional areas. Percent elongation at break was expressed as

the percentage of change of the original length of a specimen between grips at the break [26].

### Transparency and Opacity

Similarly to our previous publication [22], the color analyses of the composite bioplastics were determined using a Hunterlab colorimeter Miniscan EZ (Murnau, Germany), adopting L\* (luminosity), a\* (redness) and b\* (yellowing), which were analyzed by CIELab scale [27].

Transparency and opacity were determined to cut rectangular strips of the samples, with a size of 0.8 × 30 mm, adhered to the internal quartz cuvette wall and transmittance was read in the range of 200–800 nm (UV–VIS spectrophotometer from Varian, model Cary 1E, California, USA), using an empty cuvette as control [7, 28]. The transparency was calculated using Eq. 1:

$$\text{Transparency} = 1/(A_{500}/t), \quad (1)$$

where  $A_{500}$  = absorption at 500 nm and  $t$  = bioplastic thickness in mm.

Apparent opacity was determined on the same spectrophotometer, according to the methodology previously described [22, 29]. The absorbance at 500 nm was read for each bioplastic and the opacity was calculated according to Eq. 2:

$$\text{Opacity} = (A_{500}/t), \quad (2)$$

where  $A_{500}$  = absorption at 500 nm and  $t$  = bioplastic thickness in mm.

The humidity was determined in an oven at 105 °C (~4 h), according to the methodology of the Rocha et al. [29].

### Biodegradation Assay and Antifungal Activity

The fungicidal action tests were performed by simply observing the materials. Biodegradation assay of the starch-based bioplastic was performed similarly to our previous

publication [22]. The composite bioplastics were cut into  $4 \times 10$  cm pieces ( $40 \text{ cm}^2$  area) and packed into voil bags with four pieces of each sample per bag ( $n=4$ ). They were then buried in a garden area in the IF SERTÃO-PE, Petrolina-PE campus, in-depth of 20 cm of the soil. Samples began to be dug up and observed periodically, every 48 h, for 2 weeks. From the third week, the frequency of observations was reduced to weekly. The total period of observation was 40 days, and the term was defined according to the degradation state of the bioplastic. The observations were made based on the bioplastic area and completed when the samples decreased their area and degraded. The evaluation of the decomposition of the residues followed the simple exponential model [30], using Eq. 3:

$$X_t = X_0 \cdot e^{-kt}, \quad (3)$$

where  $X_t$  = amount of dry matter remaining after a period of time  $t$ ;  $X_0$  = amount of initial dry matter;  $k$  = decomposition constant;  $t$  = time in days. By rearranging the terms of this equation, it is possible to calculate the constant or value decomposition  $k$ , Eq. 4:

$$k = \ln(X_t/X_0)/t \quad (4)$$

The half-life is another important parameter in the evaluation of the decomposition of plant residues, expressing the period, in days, necessary for half of the material to decompose, or for half of the nutrients contained in the residues to be released. According to Rezende et al. [31], it is possible to calculate the half-life time through Eq. 5:

$$t^{1/2} = \frac{\ln(2)}{k}. \quad (5)$$

## Results and Discussion

### Physical and Mechanical Characterization

The initial properties analyzed after the preparation of the polymeric films were their transparency and color since these can be used to store food that the visual aspect is extremely important [32].

The color properties, transparency, and apparent opacity are shown in Table 2. All the bioplastics were transparent according to their  $L^*$  values ( $\sim 90\%$ ). The samples showed  $a^*$  values of around zero; thus, the influence of this parameter on the color of the bioplastics is not significant. The parameter  $b^*$  indicates a tendency towards a yellow coloration. This effect was more marked in potato starch films (higher positive  $b^*$  values), also observed with the naked eye (Fig. 1).

The transparency values of all corn starch-based films with the addition of silica powder were lower than those

**Table 2** Color properties, transparency (T) and opacity apparent (OPA) of the bioplastics prepared with corn starch (CS) and potato starch (PS)

Bioplastics	Color			T	OPA
	$L^*$	$a^*$	$b^*$		
CS1	88.97	− 1.36	10.98	2.04	0.49
CS5-P0.5	88.54	− 1.98	5.25	1.28	0.78
CS5-P1.0	90.79	− 2.00	11.76	0.68	1.46
CS5-P1.5	89.39	− 2.34	12.34	0.56	1.77
CS7.5-P0.5	87.32	0.06	1.68	1.26	0.79
CS7.5-P1.0	89.62	− 1.65	10.46	1.59	0.63
CS7.5-P1.5	88.58	− 1.74	10.50	1.41	0.71
PS1	90.41	− 0.61	11.19	0.84	1.19
PS5-P0.5	86.53	0.68	6.00	1.76	0.85
PS5-P1.0	87.50	− 1.01	17.84	0.49	2.05
PS5-P1.5	89.04	− 1.08	13.77	0.32	3.14
PS7.5-P0.5	87.76	1.175	− 1.39	1.12	0.89
PS7.5-P1.0	88.14	− 0.98	14.41	1.18	0.85
PS7.5-P1.5	86.58	− 1.22	13.39	0.78	1.28

$L^*$  = luminosity,  $a^*$  = represent redness and  $b^*$  = represent yellowing; T = transparency ( $\lambda = 500 \text{ nm}$ ); OPA = opacity apparent ( $\lambda = 500 \text{ nm}$ )

observed in the control bioplastic (CS1). For potato-starch based bioplastics, the transparency values of three samples (PS5-P0.5, PS7.5-P0.5 and PS7.5-P1.0) were higher than the value of the control sample (PS1) and of the other three samples (PS5-P1.0, PS5-P1.5 and PS7.5-P1.5) were lower than the value of the control sample (PS1). The bioplastics, CS5 and PS5, with glycerol 5% showed a decrease of transparency with increasing silica content. In general, corn starch-based bioplastics were more transparent than potato starch-based bioplastics. The opacity ranged from 0.49 to 1.77 for corn starch-based films and 0.85–3.14 for potato starch-based bioplastics, therefore, potato bioplastics are more opaque than corn bioplastics. The incorporation of silica powder increased the opacity of bioplastics containing glycerol 5%. These values were lower than those found by Coelho et al. [32] in starch-based nanocomposite films with cellulose nanocrystals from grape pomace.

The thickness and the humidity of the bioplastic are variables that influence its flexibility, mechanical and barrier properties [33, 34]. The effect of the addition of silica powder on the humidity, thickness, tensile strength, and elongation at break of bioplastics are shown in Fig. 2.

The thickness (Fig. 2 (green curve “triangle”)) of the CS and PS bioplastics varied from 0.55 to 0.61 mm and from 0.44 to 0.76 mm (glycerol 5.0%) and varied from 0.71 to 0.77 mm and from 0.54 to 0.75 mm (glycerol 7.5%), respectively. The thickness variation is mainly attributed to the casting step; therefore, this step must be carried out with great care when preparing the composite

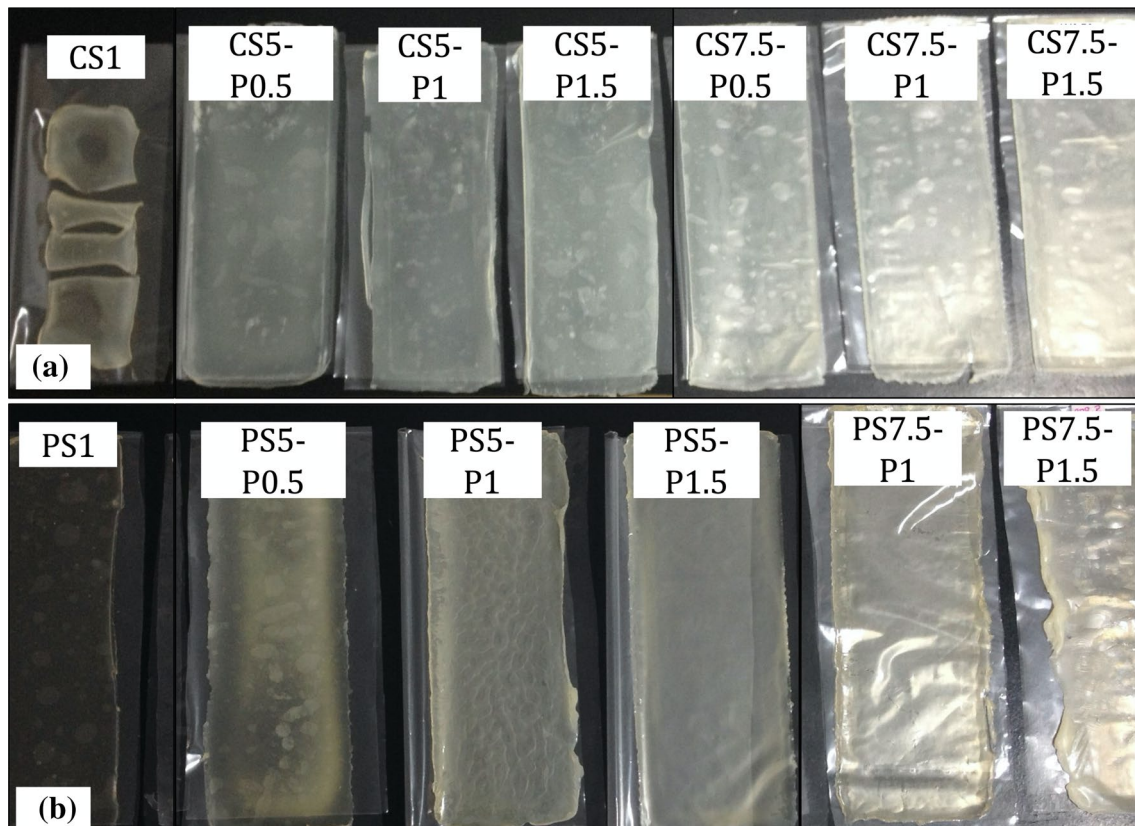


**Fig. 1** Photographs of starch-based bioplastics with 5.0 and 7.5% of glycerol and with addition of silica powder ( $P=0.5, 1.0$  and  $1.5\%$ ), **a** corn starch-based bioplastics and **b** potato starch-based bioplastics (CS1 and PS1 = control bioplastics)

bioplastics [35]. Other starch-based bioplastics presented the following thicknesses: 0.19–0.32 mm for pinhão starch [11]; 0.08–0.19 mm for corn starch; 0.06–0.21 mm for cassava starch; and 0.10–0.22 mm for wheat starch [36].

The difference in humidity content is mainly related to the composite bioplastics composition [37]. High concentrations of glycerol favor the adsorption of water molecules due to its hydrophilic nature, which retains water in the bioplastic matrix and forms hydrogen bonds (O–H). In this study, the humidity of samples ranged from 23.72 to 32.51% for CS bioplastics and from 16.19 to 31.60% for PS bioplastics (Fig. 2a–d). These humidity contents were close to those found in the literature for corn starch-based films (21–31%), cassava starch-based films (12–33%), gelatin/potato starch edible biocomposite films (15–18%) and films produced from sodium silicate extracted of rice hull ash (20–23%) [7, 9, 33, 34].

The results of the tensile strength and percent elongation at break of the starch-based bioplastics, showed that the addition of silica powder in the samples does not contribute to the increase in bioplastic tensile strength (Fig. 2 (red curve “square”)), but it significantly favored elongation at break (Fig. 2 (blue curve “ball”)).

Comparing the different contents of glycerol and silica powder for the corn starch-based bioplastic, the highest elongation at break values (Fig. 2 (blue curve “ball”)) was for the samples with 5.0% glycerol and 0.5% silica (CS5-P0.5) and with 7.5% glycerol and 1.0–1.5% silica (CS7.5-P1.0 and -P1.5). This behavior is due to the greater thickness (Fig. 2 (green curve “triangle”)) of the CS samples with 7.5% glycerol. Yao et al. [18], Wu et al. [38, 39] and Datta and Halder [21] also observed increased in the elongation at break with the addition of nanosilica powder.

For potato starch-based bioplastic, the PS1 sample showed the highest elongation at break values, and the PS7.5-P1.5 (7.5% glycerol and 1.5% silica) was obtained the elongation at break value closest to PS1 (Fig. 2 (blue curve “ball”)). The elongation at break values found in this study for corn and potato starch-based bioplastics were about 4 and 11 times higher, respectively than those found by Basiak et al. for bioplastics obtained with the same starches [40].

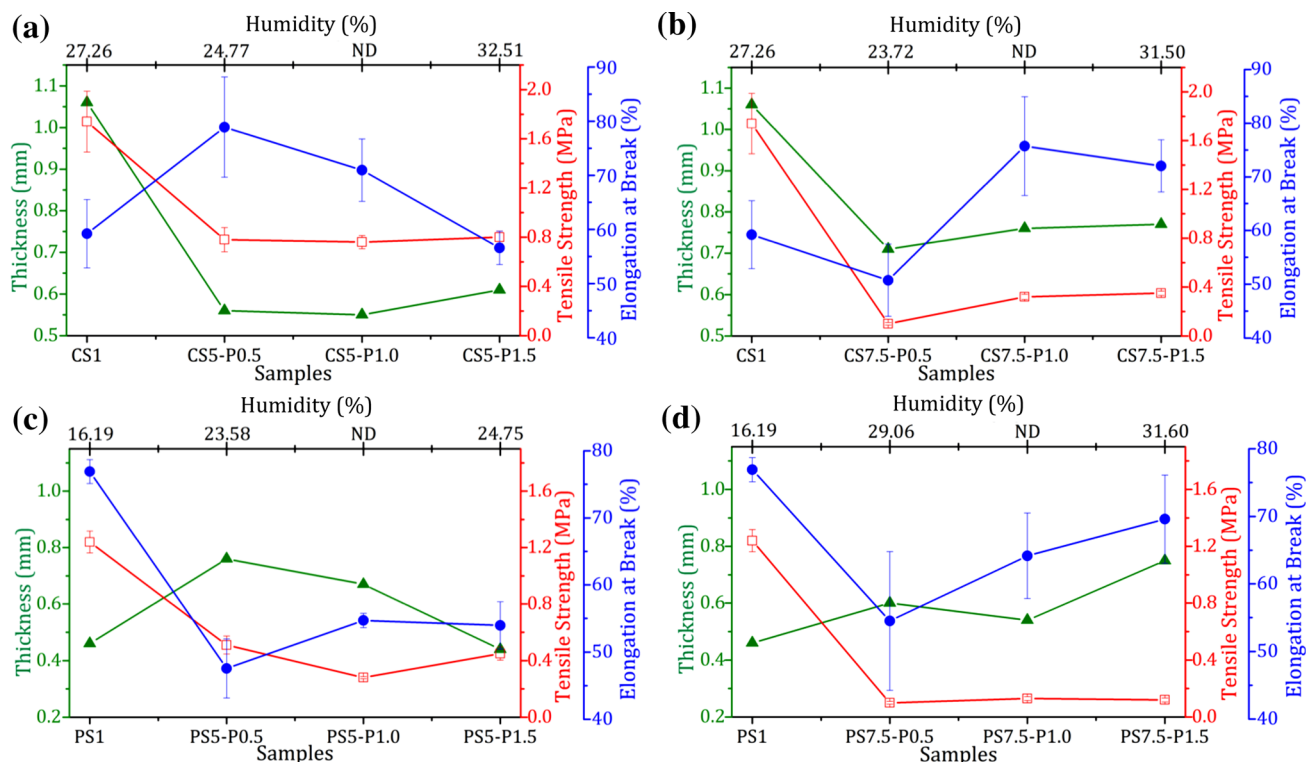


**Fig. 2** Effect of the addition of silica powder (P=0.5, 1.0 and 1.5%) on the humidity, thickness, tensile strength and elongation at break of starch-based bioplastics with 5.0 and 7.5% of glycerol. **a, b** CS = corn

starch-based bioplastics and **c, d** PS = potato starch-based bioplastics. CS1 and PS1 = control bioplastics; ND = not determined; more details in Table S1 (Color figure online)

## Structural Characterization

The FTIR spectra obtained for the silica powder and starch-based bioplastic samples obtained from the two-component mixture with glycerol are shown in Fig. 3.

Infrared spectra of the starch-based bioplastic present an intense band, at  $3285\text{ cm}^{-1}$  associated with the OH stretching referring to the hydrogen bonds (H–O...H) between the plasticizer molecules and the starch molecules and also due to the presence of water in starch-based bioplastic [10]. In all samples, except for silica, two bands of low intensity located at  $2930$  and  $2885\text{ cm}^{-1}$  are observed, these are attributed to the C–H stretching. For these same samples, except for silica, a band at  $1650\text{ cm}^{-1}$  corresponding to the  $\delta(\text{O–H})$  flexion due to the tightly bound water is observed [41].

A medium intensity band is observed at  $1370\text{ cm}^{-1}$  for the starch-based bioplastic and is attributed to bending of the  $\text{CH}_2$  and C–OH groups. The  $1150$  and  $1079\text{ cm}^{-1}$  bands observed for the starch-based bioplastic samples correspond to the C–O stretch vibration in C–O–H groups and the  $1110\text{ cm}^{-1}$  band observed only for starch-based bioplastic samples is attributed to C–O stretch vibration in C–O–C groups [41]. These results corroborate with those observed by Dang and Yoksan [27].

According to Shi et al. the bands at  $1040$  and  $1025\text{ cm}^{-1}$  are sensitive to the amount of ordered or crystalline starch and related to amorphous starch, respectively [22, 42].

For the silica three characteristic bands are observed; at  $800$  and  $450\text{ cm}^{-1}$  due to Si–O–Si symmetric stretching and at  $1060\text{ cm}^{-1}$  attributed to Si–O–Si asymmetric stretching [43]. It can be highlighted that is possible to observe only in concentrations above 1.0% of silica the signs of stretching of the Si–O–Si group are observed.

The two low-intensity bands at  $925$  and  $850\text{ cm}^{-1}$  observed in the spectra are characteristic absorption bands of anhydroglucose ring stretching vibrations of the starches structure [41]. The band at  $925\text{ cm}^{-1}$  is attributed to skeletal mode involving  $\alpha$ -1,4- glycosidic linkage (C–O–C) and the band at  $570\text{ cm}^{-1}$  is attributed to skeletal modes of pyranose ring [44].

## Thermal Stability

Thermal analyses performed by Differential Scanning Calorimetry are shown in Fig. 4. The results of the thermograms exhibited a single endothermic peak, which indicated the homogeneity of the hybrid films [11]. The crystallization temperature ( $T_{\text{peak}}$ ) obtained in this work ranged from  $122.8$  to  $157.6\text{ }^\circ\text{C}$  for CS samples and ranged from  $107$  to  $142.2\text{ }^\circ\text{C}$

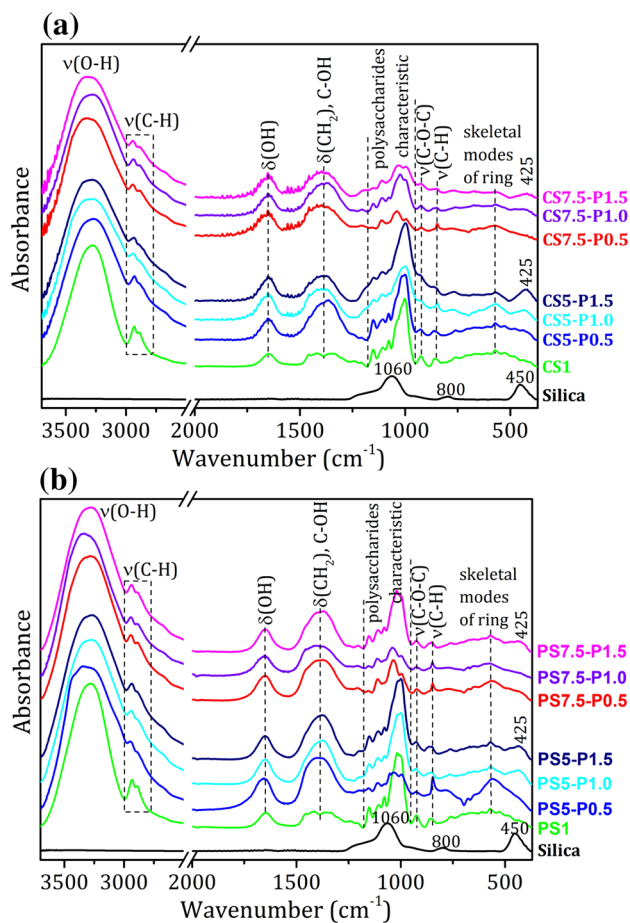


**Fig. 3** Spectra of silica and starch-based bioplastics with 5.0 and 7.5% of glycerol and with addition of silica powder (P=0.5, 1.0 and 1.5%), **a** CS samples and **b** PS samples (CS1 and PS1=control bioplastics)

for PS samples. The values found in this study were similar to those found by Pankaj et al. for corn starch films [41].

Samples of corn starch-based bioplastics showed an increase in crystallization temperature with the addition of silica powder from 122.80 °C (CS5-P0.5) to 138.85 °C (CS5-P1.5) when the glycerol content was 5.0% and decrease from 154.03 °C (CS7.5-P0.5) to 151.32 °C (CS7.5-P1.5) when the glycerol content was 7.5% (Fig. 4a). On the other hand, the samples of potato starch-based bioplastics PS5-P1.5 and PS7.5-P1.5 did not show an increase of the crystallization temperature with the addition of silica powder (Fig. 4b) due to the fact that potato starch has a much higher content of amylopectin (highly branched structure) than corn starch. Analyzing the results obtained the ideal content of silica powder to obtain a bioplastic with higher thermal resistance was 1.5% for CS and 0.5% for PS, both with 5.0% glycerol. The thermograms of samples obtained with added silica powder also revealed that the corn starch-based bioplastics were more thermally resistant when compared to potato starch-based bioplastics.

## Morphological Characteristics

SEM images are shown in Fig. 5 and confirmed that plastification and processing completely modified the structure of the starches.

The morphology of the bioplastics PS5-P1.5 and PS7.5-P1.5 was similar to sweet potato starch bioplastic [45], and the morphology of the bioplastics CS5-P1.5 and CS7.5-P1.5 was similar to corn starch bioplastic and corn starch/chitosan film [46]. The CS5-P1.5 bioplastic showed a more homogeneous matrix compared with CS7.5-P1.5, PS5-P1.5, and PS7.5-P1.5. According to Li et al. satisfactory mechanical properties are expected, corroborating with the results obtained in Fig. 2, where the CS5-P1.5 presented the highest value of tensile strength [22, 45].

## Biodegradability Assay and Antifungal Activity

The biodegradability assay of the corn and potato starch-based bioplastics was accompanied by the measurement of the area of the material. Figure 6 show CS bioplastics before (a) and after (b) biodegradability test and PS bioplastics before (d) and after (e) biodegradability test; and degradation curves of CS (c) and PS (f) samples.

The potato and corn starch-based bioplastics were degraded in 5 (f) and 39 (c) days, respectively. The degradation time of the corn starch bioplastics was similar to those found in the literature for cassava, wheat, and corn starch-based films [36, 47].

The half-life times of the starch-based bioplastics submitted to the biodegradability test were shown in Table S3. The values show that the presence of silica powder in the corn starch-based bioplastics induces the reduction of its half-life time from 22.5 days (CS1) to 19.2 days (CS5-P1.5) and 15.2 days (CS7.5-P1.5). For the potato starch-based bioplastics the half-life time was short for all samples ranged from 2.53 to 3.05 days. On the other hand, Yao et al. reported that the addition of silica nanoparticles has no significant influence on the biodegradability of bioplastics [18].

The results of the biodegradability study corroborate with the DSC thermal analyses (Fig. 4), where the corn starch-based bioplastics were more thermally resistant when compared to potato starch-based bioplastics, indicating that CS bioplastics are less biodegradable than PS bioplastics.

The silica has antifungal activity, as shown by Capeletti et al. [48] and Derbalah et al. [49]. In the present study, we observed that the addition of the silica powder to bioplastics inhibited the growth of fungi. In the absence of silicate and silica powder (CS1 and PS1), there was fungus growth (black dots) as shown in Fig. 7. This result corroborates with

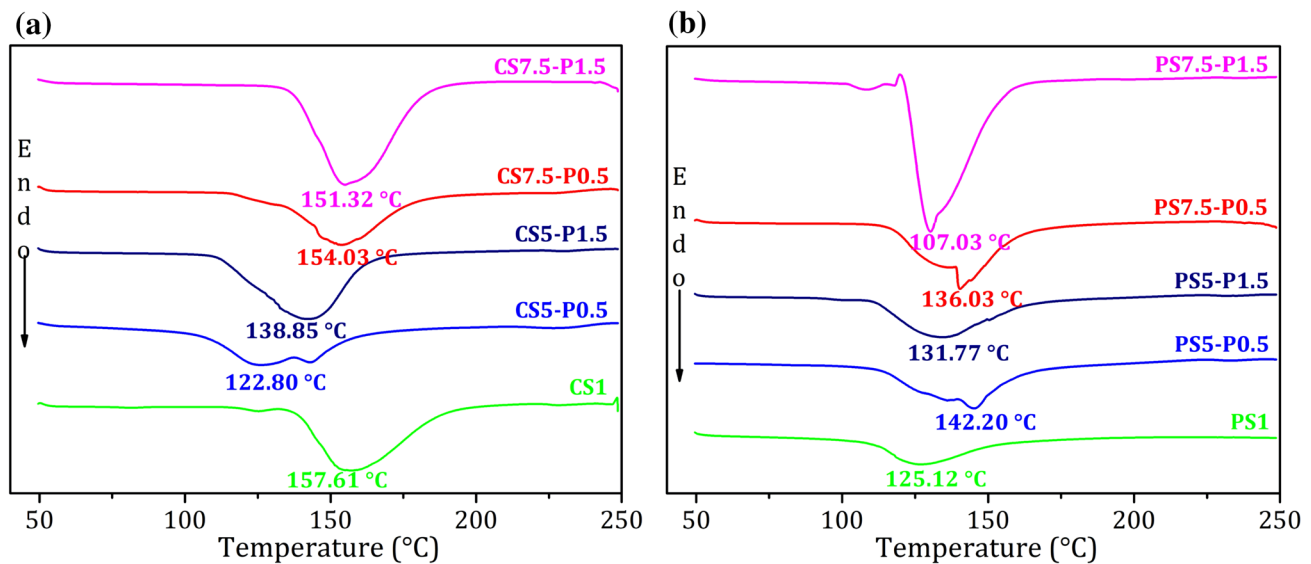


**Fig. 4** DSC curves of starch-based bioplastics with 5.0 and 7.5% of glycerol and with addition of silica powder (P=0.5 and 1.5%), **a** CS samples and **b** PS samples (CS1 and PS1 = control bioplastics) (more details in Table S2)

those found by Derbalah et al. in which mesoporous silica nanoparticles presented antifungal activity against the early blight of tomato [49]. Zhang et al. observed that the addition of silica nanoparticles in potato starch films exhibited good antibacterial activity against *E. coli* [5].

## Conclusion

The bioplastics obtained from corn starch are more transparent and less opaque than obtained from potato starch. This behavior occurs because corn starch has a higher amylose content (linear structure) than potato starch, while this last one has the highest amylopectin content (highly branched structure).

The addition of silica powder, derived from a renewable source, improved the elongation at break of the corn starch bioplastics and increased the thermal resistance of potato starch bioplastics.

The corn starch-based bioplastic obtained with 5.0% of glycerol and 0.5% of silica powder (CS5-P0.5) presented the highest percentage of elongation at break among the studied samples, increased from 59.2% (without silica powder) to 78.9% (with silica powder). On the other hand, the potato

starch-based bioplastics showed a decrease in the values of elongation at break with the incorporation of silica powder.

The thermal stability of potato starch bioplastics increased by 17 °C (PS5-P0.5) and 11 °C (PS7.5-P0.5) with the incorporation of 0.5% silica, but with the increase of silica to 1.5% thermal stability decreases, since with higher concentrations of inorganic material, there is less interaction between the polysaccharide chains of the starch, leading to decreased thermal stability.

In the biodegradability assay, the addition of powdered silica in composite bioplastics induced a reduction in half-life time. Although the potato starch-based bioplastic had worse physical, mechanical, and thermal properties, it presented higher biodegradability than corn starch-based bioplastic. The composite bioplastics of potato starch were biodegraded in 5 days, and those of corn starch took almost 40 days.

Conclusively, the addition of silica powder from sugarcane waste ash inhibited fungal growth for both corn starch and potato starch bioplastics. The produced starch-based bioplastics can be studied to use the biodegradable packaging with antifungal activity.

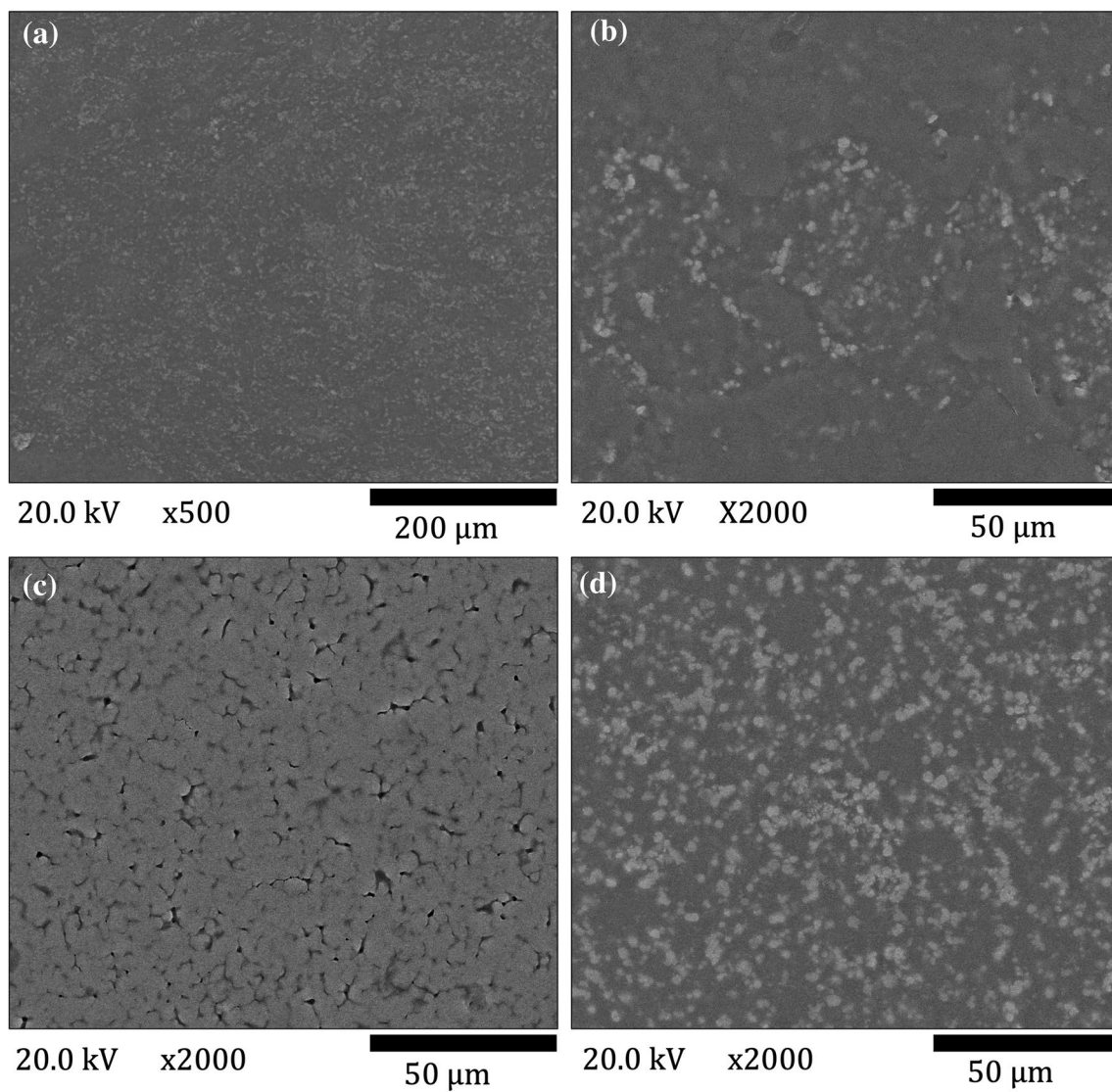


**Fig. 5** SEM images of starch-based bioplastics with 5.0 and 7.5% of glycerol and with addition of 1.5% of silica powder, **a** CS5-P1.5, **b** CS7.5-P1.5, **c** PS5-P1.5 and **d** PS7.5-P1.5 (see SEM image of silica powder in Fig. S1)

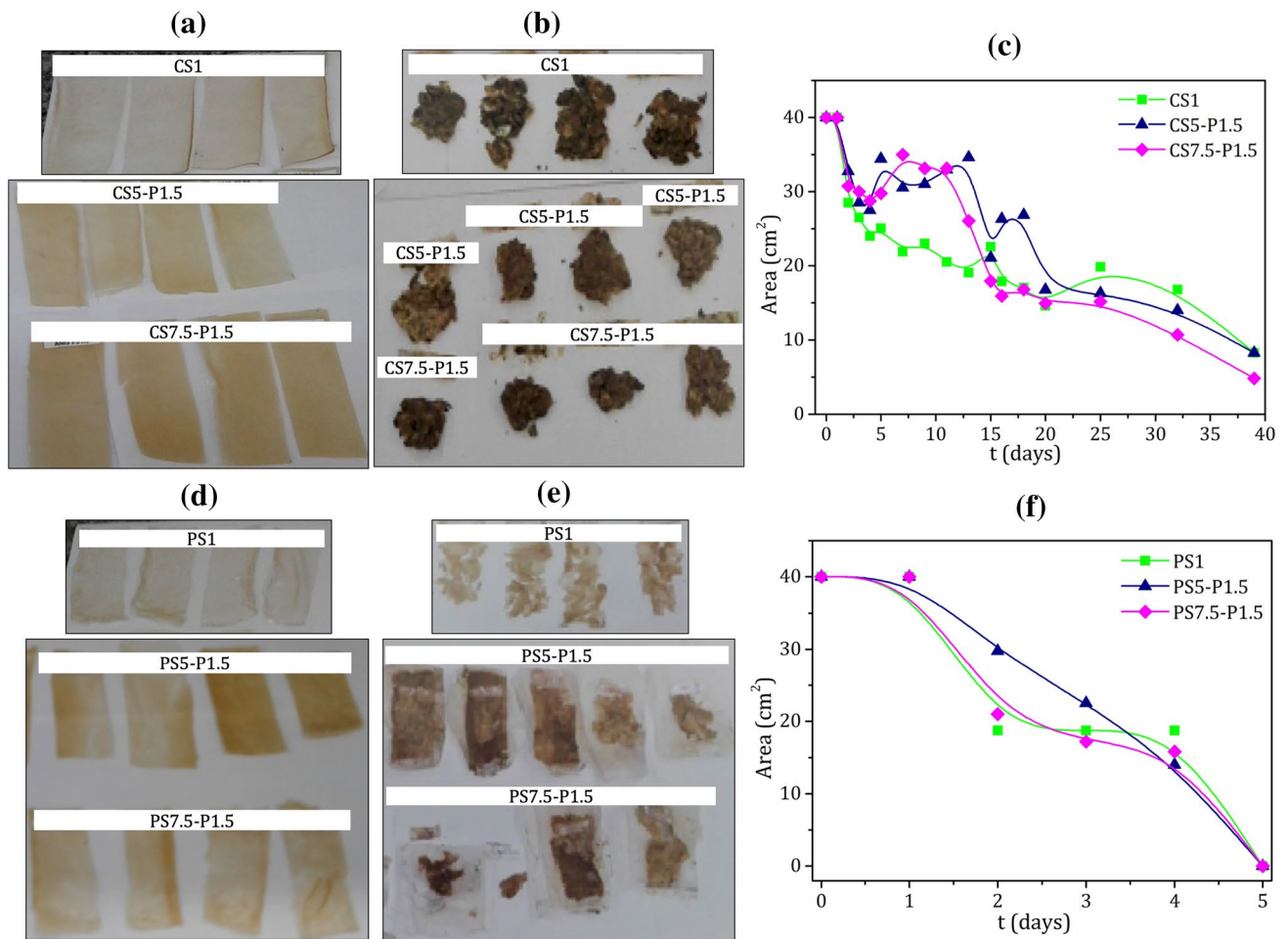


**Fig. 6** Biodegradability assay images and degradation curves of the corn and potato starchbased bioplastics with 5.0 and 7.5% of glycerol and with addition of silica powder 1.5%. **a** day 0 of CS samples, **b** end of the degradation period (day 39) of CS samples, **c** degrada-

tion curves of CS samples, **d** day 0 of PS samples, **e** end of the degradation period (day 5) of PS samples and **f** degradation curves of PS samples (CS1 and PS1 = control bioplastics)

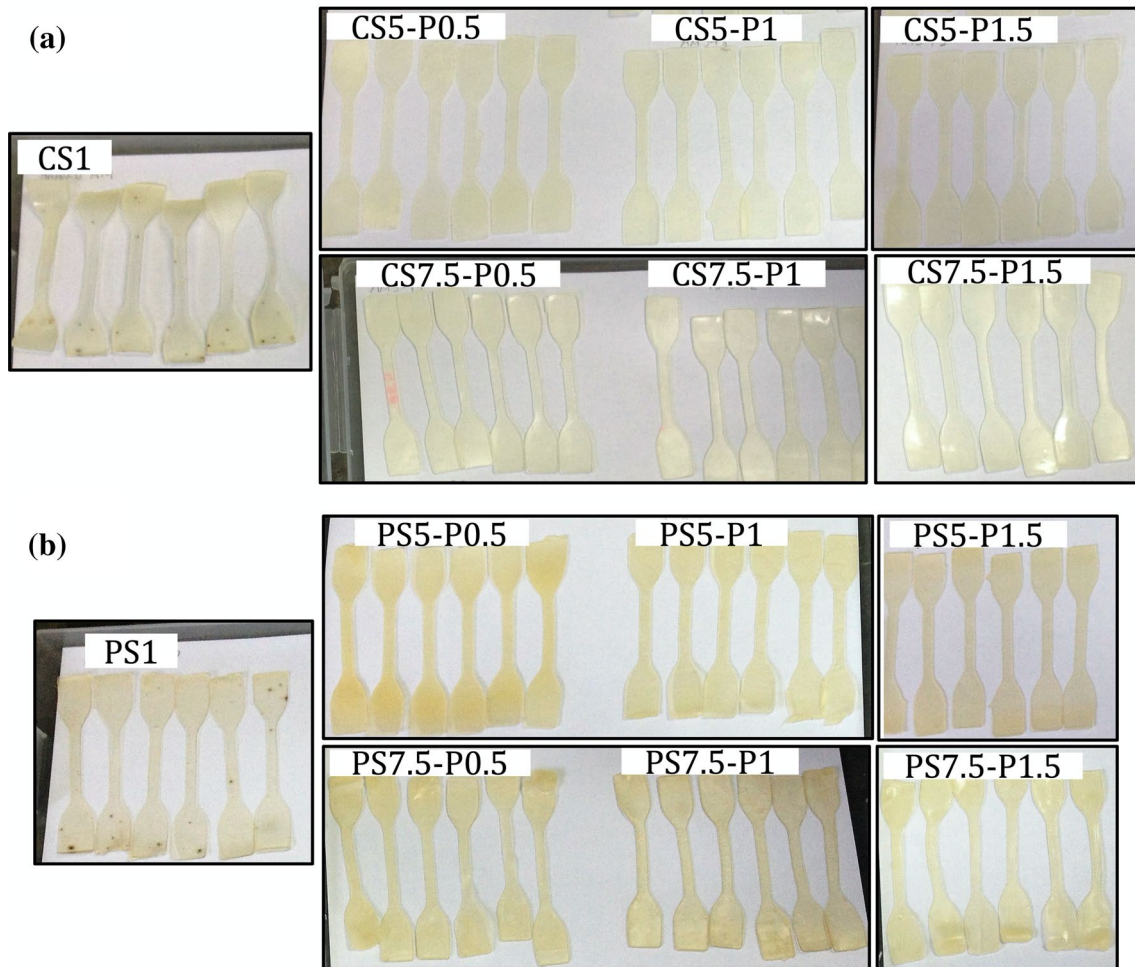


**Fig. 7** Photographs of starch-based bioplastics with 5.0 and 7.5% of glycerol and with addition of silica powder ( $P=0.5, 1.0$  and  $1.5\%$ ), **a** CS samples and **b** PS samples. Fungal growth in control bioplastics (CS1 and PS1)

**Acknowledgements** This study was financed in part by the Coordenação de Aperfeiçoamento de Pessoal de Nível Superior—Brazil (CAPES)—Finance Code 001, in part by the Conselho Nacional de Desenvolvimento Científico e Tecnológico—Brazil (CNPq), and in part by the Fundação de Amparo à Pesquisa do Estado de São Paulo—Brazil (FAPESP). The authors also are grateful to COSAN S.A. (São Paulo, Brazil) for supplying the sugarcane waste ash, the Dra. Paola Corio who made the Spectrometer from *Bruker* to collect FTIR-ATR spectra available.

## References

1. Ghayebzadeh M, Aslani H, Taghipour H, Mousavi S (2020) Estimation of plastic waste inputs from land into the Caspian Sea: a significant unseen marine pollution. *Mar Pollut Bull* 151:110871
2. Jambeck JR, Geyer R, Wilcox C, Siegler TR, Perryman M, Andrady A et al (2015) Plastic waste inputs from land into the ocean. *Science* 347(6223):768
3. Andrady AL (2017) The plastic in microplastics: A review. *Mar Pollut Bull* 119(1):12–22
4. Gonçalves de Moura I, Vasconcelos de Sá A, Lemos Machado Abreu AS, Alves Machado AV (2017) 7—Bioplastics from agro-wastes for food packaging applications. In: Grumezescu AM (ed) food packaging. Academic Press, New York, pp 223–263
5. Zhang R, Wang X, Cheng M (2018) Preparation and characterization of potato starch film with various size of nano-SiO<sub>2</sub>. *Polymers* 10(10):1172
6. Bergel BF, da Luz LM, Santana RMC (2017) Comparative study of the influence of chitosan as coating of thermoplastic starch foam from potato, cassava and corn starch. *Prog Org Coat* 106:27–32
7. Podshivalov A, Zakharova M, Glazacheva E, Uspenskaya M (2017) Gelatin/potato starch edible biocomposite films: correlation between morphology and physical properties. *Carbohydr Polym* 157:1162–1172
8. Souza AC, Benze R, Ferrão ES, Ditchfield C, Coelho ACV, Tadini CC (2012) Cassava starch biodegradable films: influence of glycerol and clay nanoparticles content on tensile and barrier properties and glass transition temperature. *LWT Food Sci Technol* 46(1):110–117
9. Luchese CL, Spada JC, Tessaro IC (2017) Starch content affects physicochemical properties of corn and cassava starch-based films. *Ind Crops Prod* 109:619–626

10. Wang C-z, Li F-y, Wang L-m, Li J-f, Guo A-f, Zhang C-w et al (2015) Research on thermoplastic starch and different fiber reinforced biomass composites. *RSC Adv* 5(62):49824–49830
11. Luchese CL, Frick JM, Patzer VL, Spada JC, Tessaro IC (2015) Synthesis and characterization of biofilms using native and modified pinhão starch. *Food Hydrocoll* 45:203–210
12. Abrial H, Soni Satria R, Mahardika M, Hafizulhaq F, Affi J, Asrofi M et al (2019) Comparative study of the physical and tensile properties of Jicama (*Pachyrhizus erosus*) starch film prepared using three different methods. *Starch Stärke* 71(5–6):1800224
13. Domene-López D, Delgado-Marín JJ, Martín-Gullón I, García-Quesada JC, Montalbán MG (2019) Comparative study on properties of starch films obtained from potato, corn and wheat using 1-ethyl-3-methylimidazolium acetate as plasticizer. *Int J Biol Macromol* 135:845–854
14. Dai L, Zhang J, Cheng F (2019) Effects of starches from different botanical sources and modification methods on physicochemical properties of starch-based edible films. *Int J Biol Macromol* 132:897–905
15. Santana RF, Bonomo RCF, Gandolfi ORR, Rodrigues LB, Santos LS, dos Santos Pires AC et al (2018) Characterization of starch-based bioplastics from jackfruit seed plasticized with glycerol. *J Food Sci Technol* 55(1):278–286
16. Zhong Y, Godwin P, Jin Y, Xiao H (2020) Biodegradable polymers and green-based antimicrobial packaging materials: a mini-review. *Adv Ind Eng Polym Res* 3(1):27–35
17. Zhao X, Cornish K, Vodovotz Y (2020) Narrowing the gap for bioplastic use in food packaging: an update. *Environ Sci Technol* 54(8):4712–4732
18. Yao K, Cai J, Liu M, Yu Y, Xiong H, Tang S et al (2011) Structure and properties of starch/PVA/nano-SiO<sub>2</sub> hybrid films. *Carbohydr Polym* 86(4):1784–1789
19. Ghazihoseini S, Alipoormazandarani N, Nafchi AM (2015) The effects of nano-SiO<sub>2</sub> on mechanical, barrier, and moisture sorption isotherm models of novel soluble soybean polysaccharide films. *Int J Food Eng* 11(6):833
20. Wu M, Wang M, Ge M (2009) Investigation into the performance and mechanism of SiO<sub>2</sub> nanoparticles and starch composite films. *J Text Inst* 100(3):254–259
21. Datta D, Halder G (2019) Effect of rice husk derived nanosilica on the structure, properties and biodegradability of corn-starch/LDPE composites. *J Polym Environ* 27(4):710–727
22. de Azevedo LC, Rovani S, Santos JJ, Dias DB, Nascimento SS, Oliveira FF et al (2020) Biodegradable films derived from corn and potato starch and study of the effect of silicate extracted from sugarcane waste ash. *ACS Appl Polym Mater* 2(6):2160–2169
23. Rovani S, Santos JJ, Corio P, Fungaro DA (2018) Highly pure silica nanoparticles with high adsorption capacity obtained from sugarcane waste ash. *ACS Omega* 3(3):2618–2627
24. Rovani S, Santos JJ, Corio P, Fungaro DA (2019) An alternative and simple method for the preparation of bare silica nanoparticles using sugarcane waste ash, an abundant and despised residue in the Brazilian industry. *J Braz Chem Soc* 30:1524–1533
25. Alves RH, da Silva Reis TV, Rovani S, Fungaro DA (2017) Green synthesis and characterization of biosilica produced from sugarcane waste ash. *J Chem* 2017:1–9
26. Maeda EA, Santos AF, Silva LGA, Schön CG (2016) Chemical, physical, and mechanical properties evolution in electron beam irradiated isotactic polypropylene. *Mater Chem Phys* 169:55–61
27. Dang KM, Yoksan R (2015) Development of thermoplastic starch blown film by incorporating plasticized chitosan. *Carbohydr Polym* 115:575–581
28. El Miri N, Abdelouahdi K, Barakat A, Zahouily M, Fihri A, Solhy A et al (2015) Bio-nanocomposite films reinforced with cellulose nanocrystals: rheology of film-forming solutions, transparency, water vapor barrier and tensile properties of films. *Carbohydr Polym* 129:156–167
29. Rocha GO, Farias MG, Carvalho CWP, Ascheri JLR, Galdeano MC (2014) Filmes compostos biodegradáveis a base de amido de mandioca e proteína de soja. *Polimeros* 24:587–595
30. Thomas RJ, Asakawa NM (1993) Decomposition of leaf litter from tropical forage grasses and legumes. *Soil Biol Biochem* 25(10):1351–1361
31. Rezende CdP, Cantarutti RB, Braga JM, Gomide JA, Pereira JM, Ferreira E et al (1999) Litter deposition and disappearance in Brachiaria pastures in the Atlantic Forest Region of the South of Bahia, Brazil. *Nutr Cycl Agroecosyst* 54(2):99–112
32. Coelho CCS, Silva RBS, Carvalho CWP, Rossi AL, Teixeira JA, Freitas-Silva O et al (2020) Cellulose nanocrystals from grape pomace and their use for the development of starch-based nanocomposite films. *Int J Biol Macromol* 159:1048–1061
33. Kalapathy U, Proctor A, Shultz J (2000) Silica xerogels from rice hull ash: structure, density and mechanical strength as affected by gelation pH and silica concentration. *J Chem Technol Biotechnol* 75(6):464–468
34. Kalapathy U, Proctor A, Shultz J (2000) A simple method for production of pure silica from rice hull ash. *Bioresour Technol* 73(3):257–262
35. Jansson A, Thuvander F (2004) Influence of thickness on the mechanical properties for starch films. *Carbohydr Polym* 56(4):499–503
36. Luchese CL, Benelli P, Spada JC, Tessaro IC (2018) Impact of the starch source on the physicochemical properties and biodegradability of different starch-based films. *J Appl Polym Sci* 135(33):46564
37. Bertuzzi MA, Armada M, Gottifredi JC (2007) Physicochemical characterization of starch based films. *J Food Eng* 82(1):17–25
38. Wu J-H, Yen M-S, Kuo MC, Chen B-H (2013) Physical properties and crystallization behavior of silica particulates reinforced poly(lactic acid) composites. *Mater Chem Phys* 142(2):726–733
39. Wu J-H, Chen C-W, Kuo MC, Yen M-S, Lee K-Y (2018) High toughness and fast crystallization poly(lactic acid)/polyamide 11/SiO<sub>2</sub> composites. *J Polym Environ* 26(2):626–635
40. Basiak E, Lenart A, Debeaufort F (2017) Effect of starch type on the physico-chemical properties of edible films. *Int J Biol Macromol* 98:348–356
41. Pankaj SK, Bueno-Ferrer C, Misra NN, O'Neill L, Tiwari BK, Bourke P et al (2015) Dielectric barrier discharge atmospheric air plasma treatment of high amylose corn starch films. *LWT Food Sci Technol* 63(2):1076–1082
42. Shi R, Liu Q, Ding T, Han Y, Zhang L, Chen D et al (2007) Ageing of soft thermoplastic starch with high glycerol content. *J Appl Polym Sci* 103(1):574–586
43. Boza AF, Kupfer VL, Oliveira AR, Radovanovic E, Rinaldi AW, Meneguín JG et al (2016) Synthesis of  $\alpha$ -aminophosphonates using a mesoporous silica catalyst produced from sugarcane bagasse ash. *RSC Adv* 6(29):23981–23986
44. Wiącek AE (2015) Effect of surface modification on starch biopolymer wettability. *Food Hydrocoll* 48:228–237
45. Li J, Ye F, Liu J, Zhao G (2015) Effects of octenylsuccination on physical, mechanical and moisture-proof properties of stretchable sweet potato starch film. *Food Hydrocoll* 46:226–232
46. Ren L, Yan X, Zhou J, Tong J, Su X (2017) Influence of chitosan concentration on mechanical and barrier properties of corn starch/chitosan films. *Int J Biol Macromol* 105(Pt 3):1636–1643

47. Fahrngruber B, Fortea-Verdejo M, Wimmer R, Mundigler N (2020) Starch/poly(butylene succinate) compatibilizers: effect of different reaction-approaches on the properties of thermoplastic starch-based compostable films. *J Polym Environ* 28(1):257–270
48. Capeletti LB, de Oliveira LF, de Almeida Goncalves K, de Oliveira JF, Saito A, Kobarg J et al (2014) Tailored silica-antibiotic nanoparticles: overcoming bacterial resistance with low cytotoxicity. *Langmuir* 30(25):7456–7464
49. Derbalah A, Shenashen M, Hamza A, Mohamed A, El Safty S (2019) Antifungal activity of fabricated mesoporous silica nanoparticles against early blight of tomato. *Egypt J Basic Appl Sci* 5(2):145–150

**Publisher's Note** Springer Nature remains neutral with regard to jurisdictional claims in published maps and institutional affiliations.